THE BNL ACCELERATOR TEST FACILITY

Kenneth Batchelor
Brookhaven National Laboratory, Upton, New York 11973

Abstract

The design of the Brookhaven National Laboratory Accelerator Test Facility is presented including the design goals and computational results. The heart of the system is a radiofrequency electron gun utilizing a photo-excited metal cathode followed by a conventional electron linac. The Nd:YAG laser used to drive the cathode with 6 ps long pulses can be synchronized to a high peak power CO_2 laser in order to study laser acceleration of electrons. Current operational status of the project will be presented along with early beam tests.

Introduction

The Brookhaven National Laboratory Accelerator Test Facility[1] is a 50 to 100 MeV electron linear accelerator utilizing a high brightness, photoexcited cathode, radiofrequency electron gun[2] followed by two traveling wave accelerator sections operating in the $2\pi/3$ mode. The facility is designed to provide output beams suitable for studies of new methods of high gradient acceleration[3,4] or of state of the art free electron lasers[5] and nonlinear Compton scattering[6] radiation sources. Initially the electron gun and accelerating sections will be powered from a single klystron amplifier giving a maximum output energy of 50 MeV (see Fig. 1).

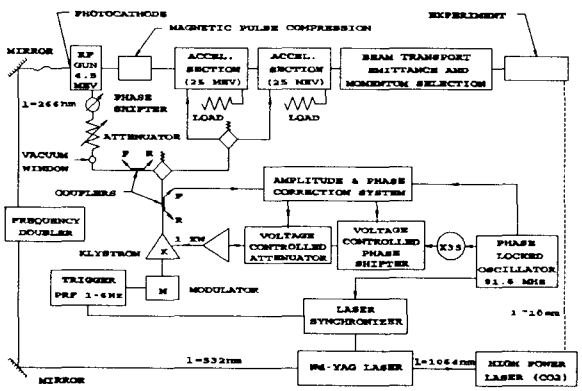

Fig. 1. Block Diagram of the Accelerator Test Facility

Design Considerations

- The electron bunch length is determined by the laser pulse width which may be small compared to the radio frequency wavelength thus eliminating the need for a buncher and permitting small energy spreads.
- The electron bunch is synchronized with the laser pulse to picosecond accuracy.
- Very low emittance beams can be produced by suitably shaping the laser pulse.
- The rf cavity can support gradients at the cathode of the order of 100 MV/m thus minimizing emittance growth due to space charge forces.
- A multicavity gun can deliver a beam of several MeV.
- The gun can operate at the same frequency as the linac.
- Optimum design of the gun cavity can minimize the emittance growth due to nonlinear components of the transverse electric and magnetic fields.

Electron Gun Design

The beam brightness is maximized by placing the cathode in the maximum electric accelerating field[7] by utilizing a half cell of a conventional disc-loaded structure followed by a suitably phased full cell (see Fig. 2). By operating in a resonant π-mode configuration and utilizing thick discs with a relatively large profile radius we are able to obtain a good approximation to the "ideal" linear dependence of the transverse fields with beam radius. By operating in π-mode and crossing the boundary between the two cells when the electric fields vanish the deflection of the beam as the bunch nears this boundary is cancelled by the opposite fields encountered as it enters the next cell. This condition determines the time at which the laser pulse should strike the cathode relative to the rf wave for minimum emittance at the gun output. Since there is no compensation for the transverse deflection at the exit of the gun essentially all of the rf induced emittance growth occurs there. The rf power is coupled to the two cells at the outer cylinder wall so that only the π-mode is coupled. The rf gun design parameters are given in Table I.

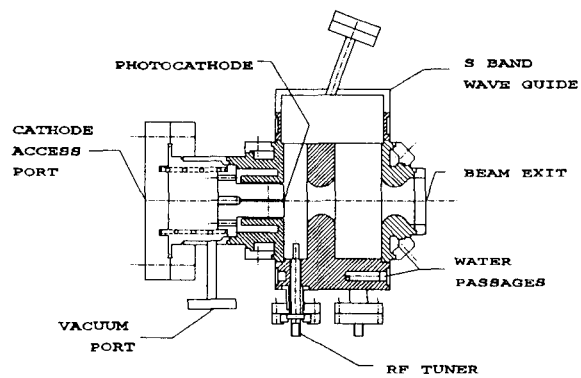

Fig. 2. Diagram of the Electron Gun

Table I. RF Gun Design Parameters

Structure type	Resonant (π-mode)
Structure inner diameter, mm	83.08
Structure length, mm	78.75
Number of cells	1+1/2
Operating frequency, GHz	2.856
Beam energy, MeV	4.65
Beam aperture, mm	20
Shunt impedance, MΩ/m	57
Cavity Q	11,900
Max. surface electric field, MV/m	119
Average accelerating gradient, MV/m	6.66
Electric field on cathode, MV/m	100
Cavity stored energy, J	4.0
Cavity peak power, MW	6.1

Photocathode Design

The photocathode requirements are as follows:

- It should have fractional picosecond response time in order to precisely follow the laser pulse form.
- It should have good quantum efficiency for operation with the laser well below damage thresholds.
- The cathode material should be robust, have good mechanical and chemical stability, and long lifetime.
- The work function should be close to and less than the photon energy of the laser.

We have chosen either a copper or yttrium metal cathode for our initial tests. Using an yttrium cathode with a work function of about 3.1 eV as compared to 4.65 eV light from a frequency quadrupoled Nd:YAG laser, the photoelectrons can emerge with up to 1.5 eV energy. If the electrons are emitted with an isotropic angular distribution at the cathode this would lead to an initial invariant emittance of 3.5π mm mrad; whereas a copper cathode with a work function of 4.3 eV would contribute a lower initial emittance but would offer a lower quantum efficiency.

Simulations of Gun Performance

The emittance of the beam from the gun has been calculated with a version of PARMELA, modified to include ejection of low energy electrons from a photocathode by a laser pulse. For electrons emitted randomly with an energy spread of a fraction of an eV, with isotropic directions and with a beam profile that is gaussian in both radius in time, as for a typical laser pulse the results are summarized in Table II for the optimized case. We use the invariant emittance, ϵ_x, defined at the bottom of this table. For these calculations the rf fields were taken from a SUPERFISH calculation and the effect of Coulomb interactions (space charge or self fields) is calculated with a point-by-point code. The effect of image charges in the cathode plane is included. The transverse and longitudinal phase space plots are given in Figures 3 and 4. It can be seen that the beam is both large in diameter and highly divergent at the gun exit.

Table II. Emittance Parameters

Laser spot radius (σ in mm)	3
Laser pulse width (σ in mm)	0.6
Charge in bunch (n Coulomb)	1
ϵ_x† at cathode (mm mrad)	3.5
$\Delta\epsilon_x$ due to self fields	6.2
$\Delta\epsilon_x$ due to rf fields	1.4
ϵ_x at exit	7.3
Beam energy spread (σ in keV)	17
Exit bunch length (σ in mm)	0.6
Exit bunch radius (σ in mm)	4.2
Exit beam angular divergence (σ in mrad)	28

$$\epsilon_x = \frac{1}{mc}\sqrt{\langle x^2\rangle\langle xp_x^2\rangle - \langle x p_x\rangle^2} = \sqrt{\langle x^2\rangle\langle \gamma^2\beta_x^2\rangle - \langle x\gamma\beta_x\rangle^2}$$

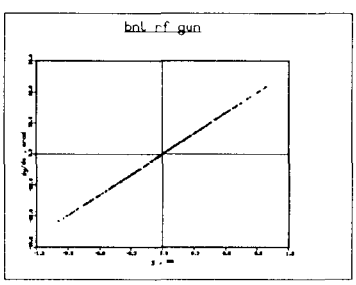

Fig.3. The transverse phase space at the gun exit for the parameters given in table II.

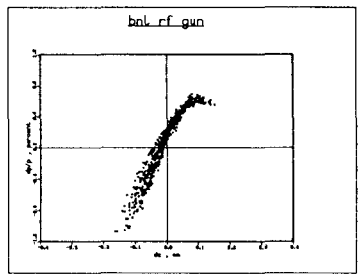

Fig.4. The longitudinal phase space at the gun exit.

Beam Transport to the LINAC

In order to allow easy access to the cathode for the photon beam it is desirable to bend the electron beam after it emerges from the electron gun. Also the longitudinal profile is such that it is possible to utilize bunch compression with a suitably designed transport system.[8] The system chosen is shown in Figure 5. It comprises two quadrupole triplets and a 180° achromatic double bend. A momentum selection slit is provided at the maximum horizontal dispersion point mid-way between the two 90° bending magnets. Provision for a vertical radiofrequency deflection device and beam profile and current measurement is also part of this arrangement.

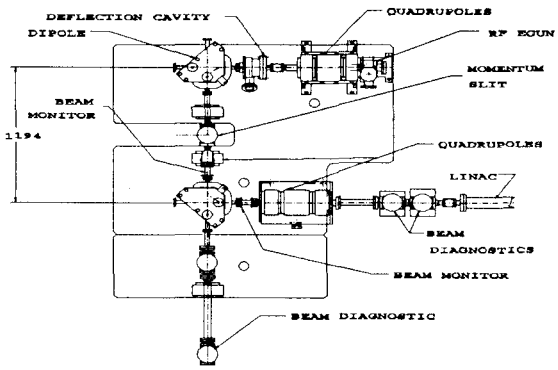

Fig. 5. Layout of the Injection System

The modeling has been done with a version of TRANSPORT with linear space charge added to study the effect of this on the beam profiles. Emittance growth in the transport line is mainly due to the following:

- mismatch caused by linear space charge forces and nonlinear space charge effects
- chromatic effects
- nonlinear magnetic fields
- spherical aberrations

The mismatch due to linear space charge can be compensated by operating the first triplet in a nonsymmetric DFD' mode. The other effects are minimized by utilizing large aperture quadrupoles with good field quality. The edges of the beam are scraped off by the beam pipe at the centers of the two quadrupole triplets at which points the pipe radius is equal to approximately 2σ horizontal beam size. The momentum slit can also be set to cut off electrons with momentum deviations down to 0.1%. For the beam parameters given in Table II and the above conditions the geometric horizontal emittance (σ) growths from 0.8 mm mrad to about 2.2 mm mrad and the vertical emittance is

preserved in passing through the transport line and about 75% of electrons with momentum deviations less then 0.4% survive.

LINAC SYSTEMS

The linac comprises two $2\pi/3$ mode, disc loaded, travelling wave sections each 3.05 meters long, excited by a single XK5 klystron delivering about 25 MW of peak power at a frequency of 2856 MHz and with a pulse duration of 3.5 μs. The rf system is designed to run at repetition rates up to 6 Hz so average power and heating is minimal. A phase locked oscillator operating at the 35th harmonic of 81.6 MHz is used to drive a series of solid state and triode amplifier stages to obtain the up to 1 KW of drive power for the klystron and also to drive and synchronize the Nd:YAG laser. A voltage controlled attenuator and phase shifter in the low level drive system may be used to vary the amplitude and phase of the radiofrequency power from the klystron during the 3.5 μs pulse. The measured bandwidth through the 1 kW stage is about 10 MHz. Amplitude stability of better than ± 0.5% and phase stability of better than 1° during a 3 μs pulse has been obtained with a preprogrammed compensation signal fed to an arbitrary function generator (see Fig. 6). Ultimately the amplitude correction signal may be obtained from a measurement of the momentum spread of the electron beam at 50 MeV and corrections applied to the subsequent pulse thus correcting for beam loading or other systematic variations during the beam macropulse. A phase correction signal from a phase comparator looking at the laser output and the klystron output may also be used for phase correction of a subsequent pulse.

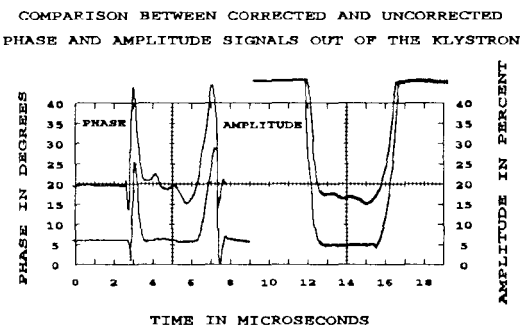

Fig. 6. Corrected Amplitude and Phase Signals at the Klystron Output

Power is fed from the klystron through a temperature controlled vacuum waveguide system using high power hybrid junctions as splitters, and phase shifters to set the correct rf phase and amplitude for acceleration. Power measurements are made with directional couplers and vacuum pumping is achieved via ion pumps connected to waveguide vacuum ports. The water cooling for the electron gun and accelerating sections is temperature controlled to 45 ± 0.02° C. Power to the electron gun is fed through a high power attenuator and phase shifter so that the power level and phase can be varied from a few KW up to a maximum of 12.5 MW.

Calculations using a modified version of the program LINAC show that for a properly matched transverse beam no increase in transverse emittance occurs in the acceleration process through the linac.

For operation in multibunch mode with 100 microbunches each separated by 12.5 ns there are a number of factors which can influence the output energy and phase spread of the electron beam[9] as follows:

a. microscopic effects within a single bunch such as:
   - rf field and phase changes during the bunch
   - longitudinal wake fields
   - space charge effects
b. macroscopic effects during a 100 bunch train of pulses such as:
   - rf field and phase changes during the macropulse due to the modulator etc.
   - input beam microbunch to microbunch energy and phase variations
   - amplitude and phase variations due to different filling times of the gun and accelerating sections
   - beam loading effects
c. macropulse to macropulse effects due to:
   - modulator pulse jitter in amplitude and time
   - temperature effects
   - laser amplitude and phase jitter

The major contribution to microscopic beam energy spread is the longitudinal wake field which for a single 6 ps bunch of 1nC charge will produce an energy charge during the pulse of about 0.4%. Proper location of the bunch centroid can reduce this wake field effect by utilizing the energy spread resulting from the rf field gradient occuring during the beam pulse.

Without correction the macroscopic effects given above, in particular beam loading effects, would produce an energy variation of about 8% during the 100 bunch macropulse. Injection phase and bunch width variations would contribute ± 0.04% energy spread in the output beam. In order to minimize amplitude and phase variations of the injected beam from the gun amplitude and phase control of the laser pulses is necessary. The final energy increases linearly with the injection energy. Changing the input phase appropriately could compensate this effect. The output energy changes nearly linearly with the square root of the input power to the accelerating sections. It is clear that the ripple during the modulator pulse must be minimized to reduce this effect. For multibunch operation with a single klystron the pulse to pulse compensation scheme proposed earlier may not be sufficient to obtain an energy spread during the 100 microbunch macropulse which is optimum for operation of a free electron laser. A second modulator and klystron allowing for separation of the electron gun and the accelerating sections is proposed for future operation of the Accelerator Test Facility.

Laser System

The laser system used for exciting the gun photocathode is a Spectraphysics CW Nd:YAG laser oscillator, mode locked to the 81.6 MHz rf reference source, with a feedback system to reduce the pulse jitter to less than 1 ps. This is followed by fiber chirping, compression and amplification stages to produce a chain of up to 200 microbunches, 6 ps long, separated by 12.25 ns. A pockels cell switching and a laser amplification system can be used to produce a single microbunch of 12 mJ energy, and of the order of 10 ps long at the laser oscillator wavelength of 1064 nm. This output is frequency doubled and then transported about 30 m to the gun hutch where a second doubling takes place. At this point there is 100 μJ of energy in a 6 ps pulse at the operating wavelength of 266 nm. This is sufficient to produce 1 nC of electron charge from the photocathode. It is also possible to produce a chain of up to 200 microbunches suitably amplified for free electron laser operation. One of the key elements in this system is a series 1000 timing stabilizer[10] purchased from Lightwave Electronics which is a phase-lock-loop feedback system for reducing pulse to pulse timing jitter, or phase noise, of the laser. The block diagram for this stabilizer is shown in Figure 7. A fast photodiode monitors a small portion of the laser output, sending this signal at the laser pulse

rate to a level detector and display and then to a precision phase detector. The phase of the laser is compared to the 81.6 MHz rf reference signal (at the same frequency). The phase detector is insensitive to laser amplitude noise, so fluctuations in its amplitude do not cause unwanted time jitter. The error signal from the phase detector is amplified and filtered before being used to drive a phase shifter that controls the timing of the mode locker drive signal. The modelocker signal is derived from a divide-by-two from the reference signal. This phase corrected signal then goes to the mode locker driver for the laser. The system has been used to reduce a timing jitter of 20 ps to less than 0.3 ps rms.

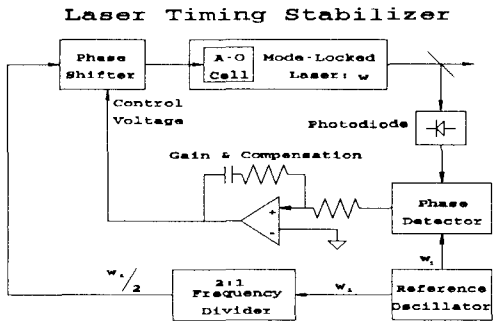

Fig.7. Phase-Lock Loop for Laser Timing Stabilization

Part of the output from the Nd:YAG at 1064 nm will be used to switch a short, synchronized CO_2 laser pulse of 6 psec duration out of a 60 ns pulse from a CO_2 oscillator by using germanium plates which change from being transmitted to reflectors when hit by 1064 nm light. A broadband CO_2 amplifier will then boost the pulse up from 10μJ to 500 mJ energy so that this may be used for laser acceleration or Compton scattering experiments.

Beam Diagnostics

ATF beam diagnostics incorporates nondestructive, strip line beam position monitors, with faraday cups for beam current measurements. Remotely insertable destructive beam profile monitors based on a phosphor screen and CCD camera system[11] are used for emittance measurement. They also give beam position information.

Momentum analysis at both 4.5 MeV and 50 MeV will be done by measuring the beam profile at the maximum dispersive points, after bending magnets. Beam profile measurement in the time domain will be done by incorporating an rf deflection cavity in the 4.5 MeV transport line and at 50 MeV by means of a fast magnetic septum pulser system and using the phosphor screen and CCD camera technique for sensing the beam.

Controls

The control system is based around a MicroVax II GPX workstation. The data acquisition and control functions use CAMAC electronics in a serial highway configuration. The control system for the ATF is built around a graphical interface and database provided by Los Alamos National Laboratory and a CAMAC driver from Kinetic Systems Corporation. All of the linac and laser systems can be driven from this system.

High Energy Beam Transport System

This system is designed to provide the desired beam parameters and beam waists at appropriate points in the three experimental beam lines and to allow for momentum analysis and transverse emittance measurements on the 50 MeV beam. The designs have been completed utilizing a version of TRANSPORT.

Operational Status

All of the electron gun and linac systems have been installed and operated at up to or close to design levels. Typical forward and reverse power waveforms for the electron gun are shown in Fig. 8 and a measured "dark current" plot for the electron gun is shown in Fig. 9. A 20 nsec pulse length excimer laser operating at a wavelength of 248 nm has been used to excite an yttrium metal cathode and the results for this mode of operation are given in Table III. The emittance measured at 3.6 MeV was less than 10 π mm mrad for a peak current of 0.6 A.

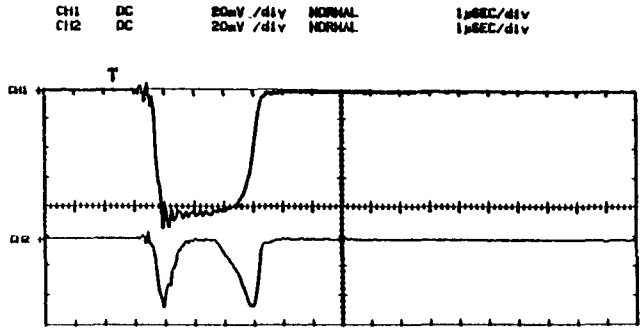

Fig.8 Forward and Reverse Power for the Electron Gun

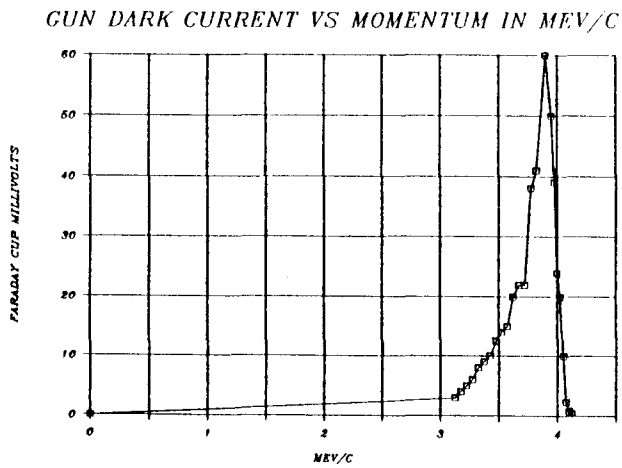

Fig.9. Measured Dark current

Table III
Brookhaven Accelerator Test Facility RF Gun Results

- 5.6 MW input RF power
- 600 μJ laser power at 248 nm
- Photo-ejected electrons accelerated to 4.2 MeV
- Measured shunt impedance = 50 MΩ/m
- dp/p = ± 0.5%
- I_{avg} = 8 mAmps
- I_{peak} = 0.6 Amps
- Initial quantum efficiency is 1.4×10^{-4}

All of the gun to linac transport elements with the exception of the vertical radiofrequency beam deflector and strip line monitors are in place and are operational from the central control computer. The magnetic components and power supplies for the high energy beam transport system are either in-house or on order. A program for measuring the magnetic field quality of all

of the transport quadrupoles is in progress. Concrete support plinths and support stands for the quadrupole magnets are already installed and the beam pipe and vacuum systems have been fabricated.

The Nd:YAG system has operated at the desired output level on the optical table in the experimental hall and the transport system and gun hutch optics are installed and operational. The CO_2 laser oscillator and amplifier systems have been delivered from Los Alamos and are being tested.

Beam studies with the electron gun and its transport system will commence as soon as operational approval has been obtained.

Experimental Area

The experimental area houses both the laser systems and the experimental beam lines. Initially two of the three beam lines shown will be implemented; namely the FEL line and the laser linac line. The first operational experiment will be the free electron laser which should give a photon source tunable over a wavelength of 500 to 1000 nm.

Future Improvements

A key element in providing a high brightness beam for the ATF experimental program is the electron gun and the transport system between it and the linac accelerating sections. Most of the emittance growth occurs at low electron energy, essentially in the first part of the first accelerating cell, and is due largely to space charge effects. A second important contribution to emittance growth is from the transport line to the linac. This growth occurs largely because of the highly divergent beam emerging from the gun giving rise to large beam radii in parts of this system. A number of corrective measures or improvements are under study as follows:

- the effect of different laser pulse longitudinal and transverse distributions on the emittance growth near the cathode.
- the effect of solenoidal focussing on the output beam divergence and emittance
- the effect of multicell gun cavities on the emittance and beam divergence
- the effect of cathode shaping
- the effect of different cathode materials on the emittance from the gun
- connecting the electron gun directly to the linac and exciting the photocathode at an angle

In addition to the gun region, for multibunch operation it will be necessary to separately control the rf amplitude and phase in the electron gun and the accelerating sections. There are plans to install a second modulator and klystron for the electron gun only and to provide for the appropriate feed forward correction scheme as provided for the accelerating sections.

Acknowledgements

The work reported results from contributions by many people who are part of the ATF design group as follows: K. Batchelor, I. Ben-Zvi, R. Fernow, J. Fischer, A. Fisher, J. Gallardo, H. Kirk, R. Palmer, Z. Parsa, J. Rogers, J. Sheehan, T. Srinivasan-Rao, T. Tsang, S. Ulc, A. VanSteenbergen, J. Veligdan and M. Woodle of Brookhaven National Laboratory; K.T. McDonald and D.P. Russell of Princeton University; C. Pellegrini and X.J. Wang of UCLA and J. Xie and R. Zhang of IHEP Beijing China. The dedicated work of our technicians, C. Biscardi, L. DeSanto, T. Monahan and H. Ratzke is also gratefully acknowledged.

References

1. K. Batchelor et al., Operational Status of the Brookhaven National Laboratory Accelerator Test Facility, Proceedings of the 1989 Particle Accelerator Conference, March 20-23, 1989, p.273.
2. K. Batchelor, H. Kirk, J. Sheehan, M. Woodle and K. McDonald, Development of a High Brightness Electron Gun for the Accelerator Test Facility at Brookhaven National Laboratory, Proceedings of 1988 European Accelerator Conference, Rome, Italy, June 2-12, 1988.
3. R.B. Palmer, A Laser Driven Grating Accelerator, Particle Accelerators 11, 81 (1980).
4. A. van Steenbergen, BNL, IFEL Demonstration Stage, BNL Report No. 42664 (1988).
5. K. Batchelor, I. Ben-Zvi, R. Fernow, J. Gallardo, H. Kirk, C. Pellegrini, A. van Steenbergen and A. Bhownik, A Microwiggler Free-Electron Laser at the Brookhaven Accelerator Test Facility, BNL Report No. 43306, 1989.
6. K.T. McDonald, Proposal for Experimental Studies of Nonlinear Quantum Electrodynamics DOE/ER/3072-38, Princeton University (Sept. 1986).
7. J.S. Fraser et al., Photocathodes in Accelerator Applications, Proceedings of the 1987 IEEE Particle Accelerator Conference, Washington D.C., March 16-19, 1987, p.1705.
8. X.J. Wang, H.G. Kirk, C. Pellegrini, K.T. McDonald and D.P. Russell, The Brookhaven Accelerator Test Facility Injection System, Proceedings of the 1989 IEEE Particle Accelerator Conference, March 20-23, 1989, p.307.
9. J. Xie and R. Zhang, Energy Spread of the ATF Beam in the Acceleration Process, BNL CAP ATF Tech Note #3.
10. M.J.W. Rodwell, D.M. Bloom and K.J. Weingarten, Subpicosecond Laser Timing Stabilization, IEEE Journal of Quantum Electronics, Vol. 25, No. 4, April 1989.
11. D.P. Russell, K.T. McDonald and B. Miller, A Beam Profile Monitor for the BNL Accelerator Test Facility, Proceedings of the 1989 Particle Accelerator Conference, March 20-23, 1989, p.1510.